

## Preparation, optimization, and characterization of simvastatin nanoparticles by electrospraying: An artificial neural networks study

Fatemeh Imanparast,<sup>1</sup> Mohammad Ali Faramarzi,<sup>2</sup> Maliheh Paknejad,<sup>1</sup> Farzad Kobarfard,<sup>3</sup> Amir Amani,<sup>4,5</sup> Mohmood Doosti<sup>1</sup>

<sup>1</sup>Department of Medical Biochemistry Faculty of Medicine, Tehran University of Medical Sciences, Tehran, Iran

<sup>2</sup>Department of Pharmaceutical Biotechnology Faculty of Pharmacy and Biotechnology Research Center, Tehran University of Medical Sciences, Tehran, Iran

<sup>3</sup>Department of Medicinal Chemistry School of Pharmacy, Shahid Beheshti University of Medical Sciences, Tehran, Iran

<sup>4</sup>Department of Medical Nanotechnology School of Advanced Technologies in Medicine, Tehran University of Medical Sciences, Tehran, Iran

<sup>5</sup>Medical Biomaterials Research Center (MBRC), Tehran University of Medical Sciences, Tehran, Iran

Correspondence to: A. Amani (E-mail: aamani@sina.tums.ac.ir) and M. Doosti (E-mail: doostimd@sina.tums.ac.ir)

**ABSTRACT:** The purpose of this study was to determine major factors impacting the size of simvastatin (SIM)-loaded poly(D, L-lactic-co-glycolide) (PLGA) nanoparticles (NPs) that was prepared using electrospraying. Three variables including concentration of polymer and salt as well as solvent flow rate were used as input variables. Size of NPs was considered as output variable. For the first time, our findings using a systematic and experimental approach, showed the importance of salt concentration as the dominant factor determining the size with a sharp and reverse effect. Optimum formulation (i.e., flow rate 0.08 mL h<sup>-1</sup>, polymer concentration 0.7 w/v %, and salt concentration 0.8 mM) was then evaluated for aqueous solubility, encapsulation efficiency, particle size, in vitro drug release pattern and cytotoxicity. A very appreciable encapsulation efficiency (90.3%) as well as sustained release profile, considerable enhancement in aqueous solubility (~5.8 fold) and high IC<sub>50</sub> (>600 μM of SIM-loaded PLGA NPs) indicated PLGA as a promising nanocarrier for SIM. The optimum formulation had particle size, zeta potential value, polydispersity index (PDI) and drug loading of 166 nm, +3 mV, 0.62 and 9%, respectively. © 2016 Wiley Periodicals, Inc. *J. Appl. Polym. Sci.* **2016**, *133*, 43602.

**KEYWORDS:** artificial neural networks; electrospraying; PLGA nanoparticles; simvastatin

Received 9 November 2015; accepted 4 March 2016

DOI: 10.1002/app.43602

### INTRODUCTION

A major limitation for a successful clinical efficacy of many drugs is inappropriate accessibility of the drug molecules to the target tissue. Therefore, designing proper methods for efficient delivery and targeting can be an ideal way to make such drugs come to market.<sup>1</sup> Nanoparticles (NPs) as smart drug delivery systems are continuously being improved to enhance their effectiveness, minimize undesirable side-effects and modify physical and chemical characteristics such as sustaining drug release and aqueous solubility.<sup>2</sup> Around 40% of drugs are either insoluble or have poor aqueous solubility. Because of their poor wetting and dissolution properties in the gastrointestinal fluids, their bioavailability following oral administration is low.<sup>3</sup> In recent years, NPs are being investigated as appropriate solutions for enhancement of solubility of such drugs.<sup>4</sup> Among various materials for preparing NPs, poly(D, L-lactide-co-glycolide) (PLGA), as a bio-degradable and biocompatible polymer, has been widely

used in drug delivery systems. PLGA has unique physical and chemical characteristics such as lack of toxicity, good tensile strength, solubility in most organic solvent, and controllable hydrophilicity for medical applications.<sup>5</sup> Various methodologies such as nanoprecipitation, solvent evaporation, emulsification/solvent diffusion, and salting out have been so far used for fabrication of NPs.<sup>6,7</sup> However, these methods have limitations including broad size distribution, difficulties in scale-up/separation process, and loss of biological functions of the drug.<sup>8,9</sup> Electrospraying (electrohydrodynamic atomization) is a simple and inexpensive technique to fabricate polymeric NPs without the limitations mentioned above. In this method, additional steps such as the need for separating the particles from solvent are eliminated.<sup>10</sup> A major advantage of this technique is that the method is very gentle, thus, commonly does not affect the biological functions of active ingredients.<sup>11</sup> Also this method takes the advantages of controlling particle size and shape by

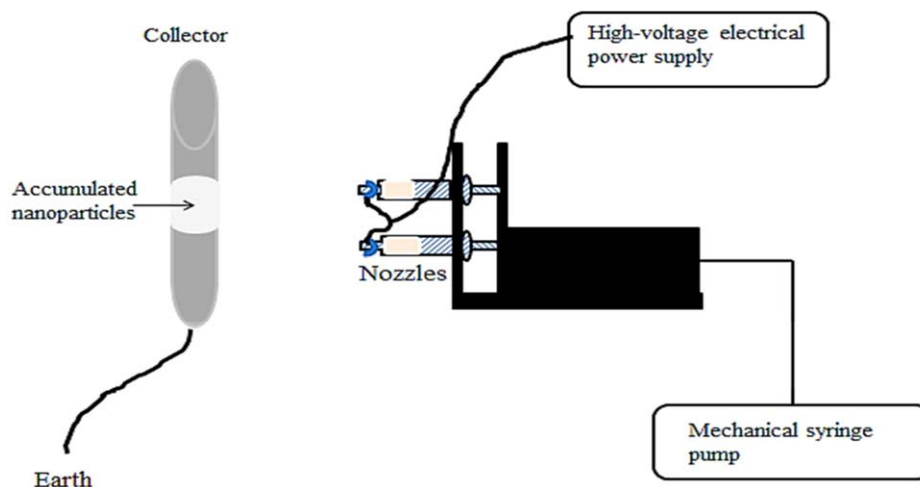


**Figure 1.** A simple diagram of the electro spraying apparatus. The spraying apparatus consisted of a high-voltage electrical power supply, a mechanical syringe pump, two stainless steel nozzles and a collector. [Color figure can be viewed in the online issue, which is available at [wileyonlinelibrary.com](http://wileyonlinelibrary.com).]

adjusting the process/formulation parameters such as flow rate, polymer concentration, type of organic salt, voltage, gauge of nozzle, and distance of nozzle to collector.<sup>12</sup>

Pleiotropic effects of statins on various diseases such as cardiovascular diseases and non-alcoholic fatty liver have been clearly established in several clinical trials.<sup>13,14</sup> Simvastatin (SIM), as a statin which is frequently used for treatment of these diseases, has poor aqueous solubility and slow rate of dissolution. Using high doses of the drug may lead to adverse effects on muscles and liver.<sup>15</sup> NPs as sustained release formulation have been reported to solve such problems.<sup>16</sup> For instance, fabricated SIM-loaded PLGA NPs by solvent displacement method have been reported to be able to increase aqueous solubility of the drug.<sup>3</sup>

Artificial neural networks (ANNs) are computer-based models that diagnose, manipulate and learn the patterns in experimental data similar to the way that the human brain does. ANNs could potentially be used to generate an appropriate model in every situation which a relationship exists between some independent variables (i.e. input parameters) and one or more dependent variable(s) (i.e. output parameter(s)).<sup>17</sup> Compared with other techniques such as response surface methodology, ANNs have shown superior performance for modeling complicated phenomena which involve non-linear relations between inputs and output(s).<sup>18,19</sup> They have successfully been used in various areas of medicine, environmental science, finance and water resources.<sup>20,21</sup>

Our previous work detailed electro spraying *N*-acetylcysteine (as a hydrophilic molecule) with PLGA. A high encapsulation efficiency (54.5%) was obtained on particle with 190-nm size, which was much higher than other conventional methods.<sup>22</sup> In this study, we aimed to set optimal formulation for synthesis of SIM-loaded PLGA NPs by electro spraying to improve aqueous solubility of SIM, a hydrophobic drug. Effect of three input (independent) factors (i.e., flow rate, concentration of polymer, and salt) on the size of NPs was assessed using ANNs modeling. Although a number of works on predicting size in electro spray

has been published (e.g., studying the effect of flow rate and polymer concentration<sup>9</sup>), majority of such studies have employed one-factor-at-a-time design. This methodology is not able to accurately estimate the effects of each factor and systematically evaluate the interactions between the factors.<sup>23</sup> Additionally and of particular interest, we studied the effect of dodecyltrimethylammonium bromide (DTAB) as a salt on altering particle, which has been rarely reported so far. A report, employing modeling methodology, indicates that increasing the concentration of a nonorganic salt (i.e., NaCl) makes the size smaller.<sup>24</sup> The only experimental work which we have found shows that smaller PLGA NPs could be synthesized in the presence of DTAB.<sup>25</sup> However, this study is also based on one-factor-at-a-time design. Additionally, only very limited data (i.e., values of 0 and 2 mM of salt) have been reported in the work.

## EXPERIMENTAL

### Materials

PLGA (50:50,  $M_w$  50,000 g mol<sup>-1</sup>, Shenzhen Esun Industrial, China), SIM crystalline powder ( $M_w$  418.56 g mol<sup>-1</sup>, Mehrdarou pharmaceutical, Iran), Acetone [99.9%, high-performance liquid chromatography (HPLC) grade, Merck, Germany], dodecyltrimethylammonium bromide (DTAB) and 3-(4,5-dimethylthiazol-2-yl)-2,5-diphenyltetrazoliumbromide (Sigma-Aldrich, USA), Dulbeccos modified eagles medium (DMEM), fetal bovine serum (FBS), phosphate-buffered saline (PBS, 0.01M, pH 7.4) and penicillin and streptomycin antibiotic mixture (Life technologies, grand Island, USA) were used in this work.

### Fabrication of SIM-Loaded PLGA Nanoparticles

SIM-loaded PLGA NPs were fabricated using double-nozzle electro spraying. The spraying apparatus consisted of a high-voltage electrical power supply, a mechanical syringe pump and two stainless steel nozzles with inner and outer diameters of 1.77 and 2.34 mm, respectively (Figure 1). SIM and PLGA were dissolved in acetone by sonicator, then, the solution was injected using the pump. Three experimental parameters including solute (polymer) concentration (0.5–0.9 w/v %), salt

**Table I.** The Training Parameters used with INForm v4.02

	No. of hidden layers	1
Network structure	No. of nodes in hidden layer	3
Backpropagation type		
Backpropagation	Momentum factor	
Parameters	Learning rate	0.700000
Targets	Maximum iterations	1000
	MS error	0.000100
	Random seed	10000
Smart stop	Minimum iterations	
	Test error weighting	
	Iteration overshoot	
	Auto weight	
	Smart stop enabled	
Transfer function	Output	
	Hidden layer	

concentration (DTAB) (0–2 mM), and flow rate (0.5–1.5 mL h<sup>-1</sup>) were varied and the corresponding variation in particle size was examined. The concentration ratio of drug to polymer was 1 to 10. Possible 40 combinations of parameters were investigated. Solutions of all combinations were electrosprayed with an applied electrical potential of 10 kV and collected at a distance of 100 mm from nozzles onto a collection drum. Prepared samples were examined to determine their particle size and morphology using SEM. The data were then employed to evaluate the impact of the variables on average size with regards to the model obtained from ANNs.

#### Artificial Neural Networks Studies

In this study, we used commercial ANNs software (INForm V4.02, Intelligensys, UK). Data from the generated model were illustrated as 3D graphs. Relations between the inputs and output were obtained by comparing the response surfaces. Input variables included polymer concentration, DTAB concentration and solvent flow rate. Average size of NPs was considered as the output variable. Forty samples were prepared having random values for the above mentioned inputs, of which, 29 were taken as training data set to train network of the relations between the inputs and the output. Three sets were used as test data to prevent overtraining during the training procedures. Remaining data were kept away from training process to evaluate the accuracy of generated model as “unseen” data. The training parameters used during the modeling procedure have been briefed in Table I.

#### Characterization of Nanoparticles

**Particle Size and Zeta Potential of Nanoparticles.** Size, polydispersity index (PDI) and zeta potential of NPs were determined by a Zetasizer (Malvern, UK). Morphology of NPs was characterized using Scanning Electron Microscope (SEM, AIS2100, Korea). Nearly 100 particles of the images obtained from each sample were used to calculate the mean diameter. SIM-loaded NPs were characterized by Fourier Transform Infra-

red Spectroscopy (FT-IR, NICOL IS10, USA). The powder was mixed with KBr to form pellet and examined in the range of 400–4000 cm<sup>-1</sup>. X-ray diffraction (XRD, Inel, EQ 3000, France) and differential scanning calorimetry (DSC, LINSEIS STA- PT 1000, USA) measurements were performed to compare the physical status of SIM in the NPs with that of pure drug and pure PLGA.

**Encapsulation Efficiency.** SIM content in PLGA NPs was investigated by dispersing 10 mg of PLGA NPs in 10 mL acetonitrile and analyzing the diluted solution by UV analysis method (LKB Ultraspec Plus, pharmacia, USA) at 238 nm.<sup>26</sup> Encapsulation Efficiency was calculated by eq. (1).

$$\text{Encapsulation Efficiency \%} = \left( \frac{\text{drug content in the NPs}}{\text{total drug content added}} \right) \times 100 \quad (1)$$

**Solubility Study of Simvastatin.** Solubility of SIM in forms of bulk and encapsulated in PLGA NPs studies were assessed in triplicate with some modification as described earlier.<sup>16</sup> Briefly, an excess amount of SIM and SIM-loaded PLGA NPs were added to 5 mL phosphate buffer solution (pH 7.4), and sonicated at room temperature for 1 h. Samples were centrifuged at 10,000 rpm for 15 min. The supernatant was diluted with methanol, then, the SIM concentration was analyzed by UV analysis at 238 nm.

**In Vitro Drug Release Studies.** In vitro drug release studies were performed with some modifications as described earlier.<sup>27</sup> Briefly, 100 mg of the SIM-loaded PLGA NPs was suspended in phosphate buffer with pH 7.4 in a mechanical shaking bath (100 cycles/min), with temperature adjusted to 37 °C. At selected time intervals, 3.0 mL of the sample was removed and centrifuged at 5000 rpm for 10 min. The precipitates were resuspended with 3 mL of fresh phosphate buffer and added to the glass bottle. Supernatants were collected and filtered through 0.45 μm membrane, and diluted and analyzed by UV-spectrophotometry at 238 nm. Experiments were performed in triplicates.

**Evaluation of Cytotoxicity.** MTT assay was used to evaluate cytotoxicity of SIM, PLGA NPs, and SIM-loaded PLGA NPs against human umbilical vein endothelial cells (HUVECs) with some modification as described earlier.<sup>27</sup> Briefly, HUVECs (5 × 10<sup>4</sup> cells/well) were seeded into 96-well plates and incubated to 70–90% confluence. Various concentrations of SIM, PLGA NPs, or SIM-loaded PLGA NPs in DMEM medium plus 10% FBS were added to each well and incubated for 24 h. Next, cells were washed twice with phosphate-buffered saline (PBS). Then, MTT (100 μL well<sup>-1</sup>) was added to each well. After incubation with MTT for 4 h, 100 μL of DMSO was added to each well. When the crystal was completely dissolved, optical density was measured at 570 nm by enzyme-linked immunoassay analyzer (ELISA) reader (Biotek, USA). Experiments were performed in triplicates.

**Statistical Analysis.** Data are expressed as mean ± standard deviation. Significance was considered as *P* < 0.05. Data were analyzed by One-way ANOVA followed by Tukey's post hoc comparison test or a Mann–Whitney test.

**Table II.** The Validation Data Sets Utilized in ANNs Modeling

Concentration of polymer (%w/v)	Solvent flow rate (mL min <sup>-1</sup> )	Concentration of salt (mM)	Average-observed (nm)	Average-predicted (nm)
0.8	0.11	1.25	276	290
0.8	0.13	0.50	261	249
0.9	0.15	1.50	256	254
0.5	0.05	1.50	200	256
0.6	0.10	0.50	207	267
0.9	0.10	0.00	487	545
0.8	0.08	2.00	278	240

## RESULTS AND DISCUSSION

### Artificial Neural Networks Studies

Subsequent to modeling the experimental data using ANNs, the model showed an  $R^2$  of 0.79 for unseen data that indicates a satisfactory predicting model (see Table II).<sup>28</sup> This model was then used for studying the impact of input variables used in this study, on size of NPs. To realize the relationships between inputs and output in an ANNs model, the first option would be use of sensitivity analyses. However, we employed response surfaces to “visualize” the interactions between the inputs and the output in this study as described previously.<sup>29,30</sup> This method, in brief, investigates the impact of two variables on the output using response surfaces provided by the software, while other variable(s) are fixed at certain values (i.e., a low, a mid-range, and a high value, respectively).<sup>18</sup>

To do so, the impact of solvent flow rate and concentration of salt on size average was investigated when concentration of polymer was fixed at low, mid-range, and high values (i.e., 0.6, 0.7, and 0.8 w/v %, respectively). From the details, no clear rule may be obtained between particle size and flow rate, while by increasing flow rate, the particle size seems to decrease, a transient but important increase in the particle size is observed from  $\sim 0.08$  to  $\sim 0.1$  mL h<sup>-1</sup> values of flow rate [Figure 2(A)]. From the literature, there is a direct relationship between the particle size and flow rate.<sup>8,9,31</sup>

$$d = \alpha \left( \frac{\rho \varepsilon_0 Q^4}{I^2} \right)^{\frac{1}{6}} \quad (2)$$

Where  $d$ ,  $\alpha$ ,  $Q$ ,  $\rho$ ,  $I$ , and  $\varepsilon_0$  are droplets diameter (m), a constant, liquid flow rate (m<sup>3</sup> s<sup>-1</sup>), solution density, current within the liquid cone and permittivity of vacuum, respectively. For instance, this effect at high values of flow rate, (from 0.15 to 2.00 mL h<sup>-1</sup>) was studied by Hartman *et al.* that showed a direct relationship between flow rate and particle size.<sup>31</sup> The inconsistency of our findings may be due to low values of flow rate (i.e., below 0.15 mL h<sup>-1</sup>). From a previous work with, under extremely low liquid flow (<0.2 mL h<sup>-1</sup>), relation between flow rate and size do not follow the eq. (2), probably due to unstable spraying procedure.<sup>32</sup> It is thus arguable that at our work, instabilities happening during spraying process lead to inability of obtaining a model to predict the NP formation.

Also, by increasing concentration of salt, the average size of particles generally decreases, especially in the region of 0–0.8 mM

of salt concentration. Our results agree with previous study indicating that increasing salt makes a significant decrease in size through enhancement of liquid conductivity.<sup>25</sup>

$$d \propto \left( \frac{1}{k} \right)^{\frac{1}{6}} \quad (3)$$

where  $d$  and  $K$  are droplets diameter and liquid conductivity, respectively.

In Figure 2(B), solvent flow rate has been fixed at low, mid-range, and high values (i.e., 0.07, 0.10, and 0.13 mL h<sup>-1</sup>, respectively) to create 3D graphs of average size against concentration of polymer and that of salt. The details show that, similar to the previous section, by increasing concentration of salt, the average size of particles decreases sharply, in particular, when salt concentration is in range of 0.0 to  $\sim 0.8$  mM. The details also indicate that change in concentration of polymer does not remarkably affect the size here in. From a previous work, in electrospraying when polymer concentration is high (>8%), increasing the polymer concentration reduces the solvent evaporation rate. Therefore, larger particles are expected to develop due to formation of a thick shell with larger diameter. However, when concentration is low (<4%), effect of increasing of polymer concentration on particles size could be ignored as the process of solvent evaporation is fast.<sup>25</sup>

Figure 2(C) illustrates the impact of solvent flow rate and concentration of polymer on the average size when the concentration of salt has been fixed in low, medium and high values (0.3, 1.0, and 1.3 mM, respectively). From the details, change in polymer concentration has no important effect on particle size. Also, the complex effect of flow rate on particle size is apparent.

To summarize, the salt concentration appears to be the dominant factor in determining size with a reverse effect especially in the low values.

### Characterization of Nanoparticles

Results of ANNs modeling showed that NPs with minimum size may be obtained at values of 0.08 mL h<sup>-1</sup>, 0.8 mM, and 0.7 w/v % for flow rate, salt concentration and polymer concentration, respectively. This sample was then experimentally prepared and the physicochemical tests were performed on the optimum sample as details below. SEM image showed smooth surface and uniform morphology of NPs (Figure 3).



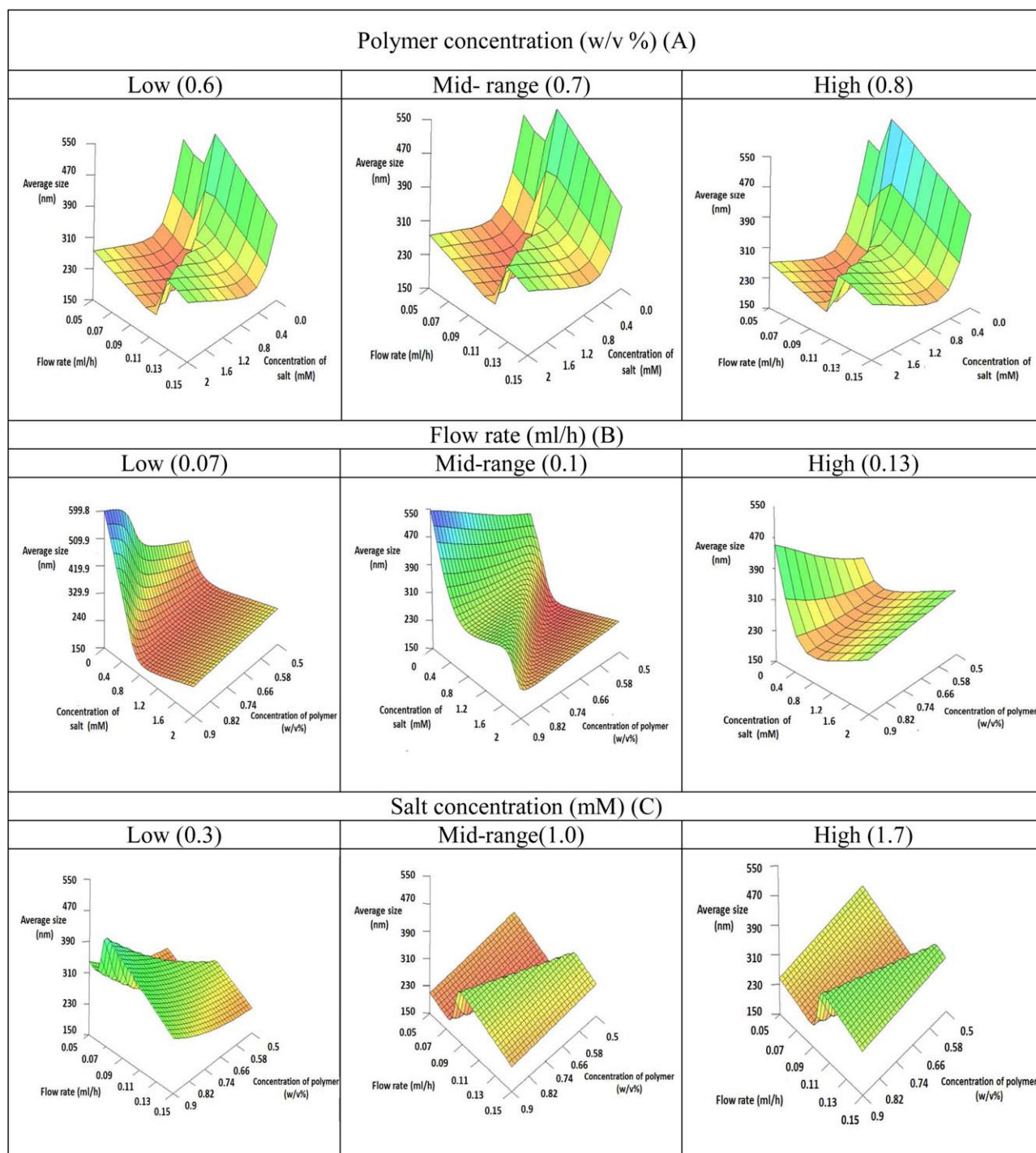


**Figure 2.** The 3D plots of average size predicted by the ANN model at low, medium, and high values of PLGA concentration, flow rate and salt concentration (A–C, respectively). [Color figure can be viewed in the online issue, which is available at [wileyonlinelibrary.com](http://wileyonlinelibrary.com).]

Particle size, zeta potential value, and polydispersity index (PDI) were found to be  $166 \pm 49$  nm, +3 V and 0.62, respectively. The cationic nature of PLGA NPs is probably due to presence of DTAB as stabilizer.<sup>33</sup>

Figure 4 shows FT-IR spectra of SIM, PLGA, and SIM PLGA samples. SIM spectrum shows peaks of free O–H stretching vibration at  $3553\text{ cm}^{-1}$ , C–H stretching vibrations at 3011,

$2959$ ,  $2872\text{ cm}^{-1}$ , and stretching vibration of ester and lactone carbonyl functional group at  $1714\text{ cm}^{-1}$ . FTIR spectrum of PLGA indicates peaks of OH stretching vibrations at  $3200$ – $3500\text{ cm}^{-1}$ , CH, CH<sub>2</sub>, CH<sub>3</sub> stretching vibrations at  $2850$ – $3000\text{ cm}^{-1}$ , carbonyl C=O stretching vibrations at  $1700$ – $1800\text{ cm}^{-1}$ , and C–O stretching vibrations at  $1050$ – $1250\text{ cm}^{-1}$ .<sup>27,34</sup> The above mentioned peaks are also clear in SIM PLGA NPs. Thus, no chemical interaction between various

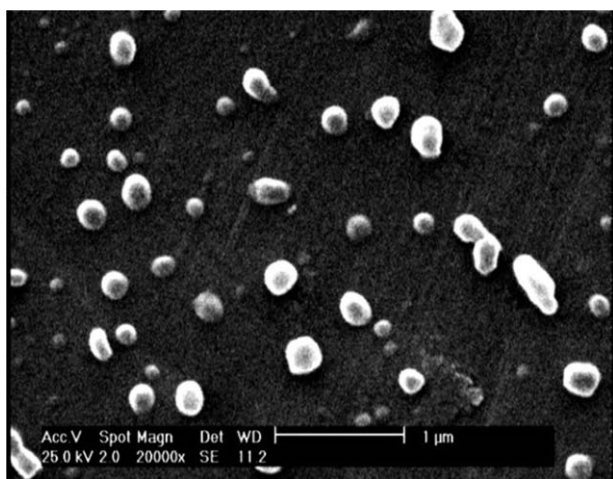


**Figure 3.** SEM image of SIM-PLGA nanoparticles, scale bar = 1  $\mu\text{m}$ .

functional groups may be detected between SIM and polymer molecules. This is expected to provide a desired pattern of drug release in a drug delivery.<sup>27</sup>

Distinct peaks in XRD spectrum of SIM at diffraction angles of  $2\theta$   $10^\circ$ – $40^\circ$  indicate that pure SIM is present in a crystalline form while a substantial reduction at diffraction angles of SIM-loaded PLGA NPs approves reduction in the crystallinity of the precipitated SIM in NPs and increase in its amorphous state. Also, distinct peaks in XRD spectrum of PLGA shows an amorphous form for the nanoparticles (Figure 5). Furthermore, SIM in its natural and crystallite state has sharp melting endotherm at  $137^\circ\text{C}$  in the DSC analysis curve. However, the original melting point of the drug disappears in encapsulated form in the PLGA, indicating the formation of an amorphous inclusion complex. It is noteworthy that a low peak close to  $50^\circ\text{C}$  is

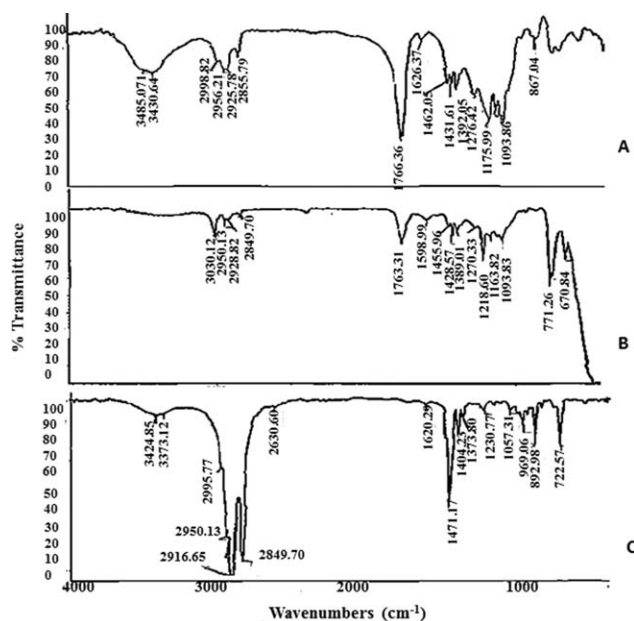


**Figure 4.** FT-IR spectra of SIM (A), PLGA (B), and SIM-loaded PLGA NPs.

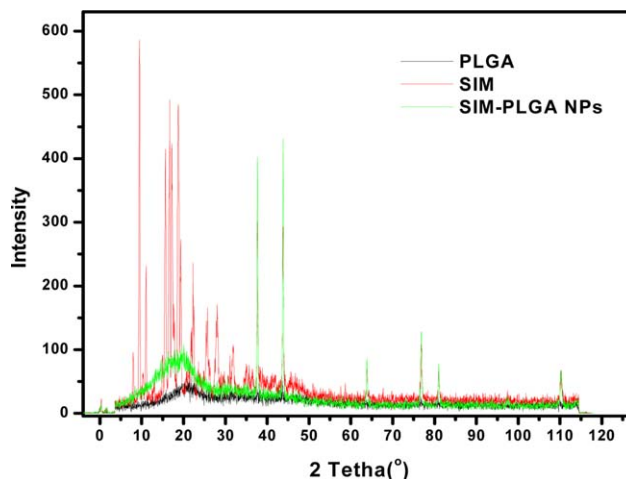


**Figure 5.** XRD spectra of simvastatin (SIM) (A), PLGA (B), and SIM-loaded PLGA nanoparticles (C). [Color figure can be viewed in the online issue, which is available at wileyonlinelibrary.com.]

probably showing glass transition temperature of PLGA (Figure 6). Overall, XRD spectra and DSC analysis curves of SIM, PLGA, and SIM-loaded PLGA NPs showed that SIM is either molecularly dispersed in the polymer or distributed in amorphous form, similar to the results of previous reports.<sup>3,27</sup>

Our solubility studies showed solubility of SIM and SIM-loaded NPs as  $22.07$  and  $127.6 \mu\text{g mL}^{-1}$ , respectively. Thus, SIM-loaded NPs made an  $\sim 5.8$ -fold increase in solubility in comparison with SIM alone. Emulsification solvent evaporation technique and nano-precipitation-solvent displacement method have been shown to be able to increase solubility of SIM-loaded NPs up to 4.8 and 5 fold, respectively.<sup>3,27</sup> As a prime advantage of electrospraying, encapsulation efficiency should be more than other methods. In this study, 90.3% of SIM was encapsulated in NPs, while this value was 46% using the water miscible solvent displacement method.<sup>35</sup>

Figure 7 shows the results of release studies. The details show an initial release (ca., 43%) within the first 13 h after maintaining the NPs in PBS, similar to study of Soni *et al.* which had an initial release of 40.56% in the first 4 h. This initial release is due to desorption of the surface-bound/adsorbed SIM. Compared with initial release of SIM microspheres (43% in the first 5 day), release from NPs is faster, probably due to the fact that the surface area of the NPs is more of microparticles. Additionally, a gradual increase in released SIM concentration with minimum fluctuations in release rate shows a homogenous distribution of SIM in NPs.<sup>27</sup>

To assess the cytotoxicity of SIM, PLGA NPs and SIM-loaded PLGA NPs by MTT assay, HUVEC cells were used. By increasing concentration of PLGA NPs and SIM-loaded PLGA NPs, cell viability decreases. However, even high concentrations of NPs; render only a small cytotoxic effect. For instance, a high concentration ( $600 \mu\text{g mL}^{-1}$ ) of PLGA NPs and SIM-loaded PLGA NPs made around 40% reduction in viability compared with the control and 20% reduction compared with  $100 \mu\text{g mL}^{-1}$  of PLGA NPs. This finding agrees with previous

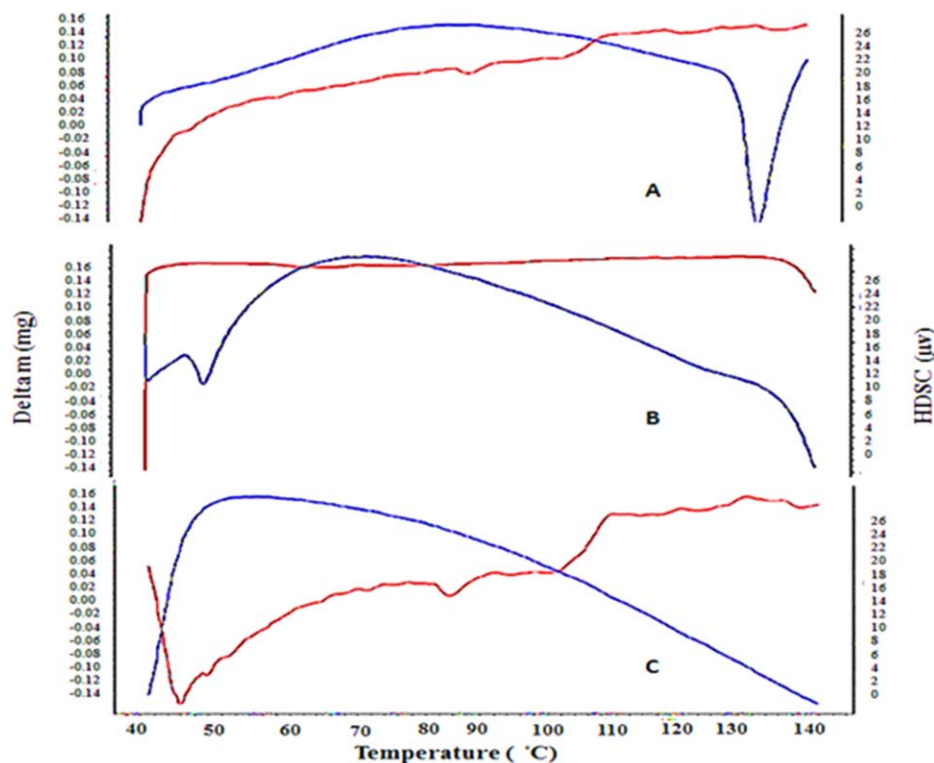


**Figure 6.** DSC analysis curve of SIM (A), poly(D, L-lactic-co-glycolide) (PLGA) (B), and SIM-loaded PLGA NPs (C). [Color figure can be viewed in the online issue, which is available at [wileyonlinelibrary.com](http://wileyonlinelibrary.com).]

studies showing that PLGA NPs is biocompatible for cells and reduction of availability is dependent on its concentration.<sup>33</sup> PLGA is converted in the body into its components include glycolic acid and lactic acid. These components are biocompatible and easily metabolized by the biochemical pathways.<sup>36</sup> Having mentioned that in our work, the decline in viability may be to some extent dependent on DTAB in NPs. Furthermore, samples with different amounts of SIM (e.g., 1, 10, 20  $\mu\text{M}$ , no PLGA) showed no significant difference in cytotoxicity profiles (Figure 8). Results of Wiesbauer *et al.* showed that SIM (5  $\mu\text{M}$ ) has no toxic effects on HUVEC,<sup>37</sup> while in another work 5 and 10  $\mu\text{M}$  concentrations of SIM significantly reduced cell viability of retinal microvascular endothelial cells.<sup>38</sup> Another more detailed work has indicated that different statins have no important

effect on viability of karyotypically normal hESCs (HES3 and BG01) even in high doses (20  $\mu\text{M}$ ). While, cell viability of abnormal hESCs (BG01V) and breast adenocarcinoma cells (MCF-7) reduced in a dose-dependent manner compared with control.<sup>39</sup> The differences observed in the results of different studies may be due to the differences in cell type, measurement techniques, and experimental conditions.

## CONCLUSIONS

The main aim of this study was to optimize an electrospray method for preparation of SIM-loaded PLGA NPs. For this purpose, effect of various parameters, including solvent flow rate, concentration of polymer, and salt concentration on size of NPs was evaluated. The dominant factor determining the size of NPs was found to be size which reduced the size by its increase. The

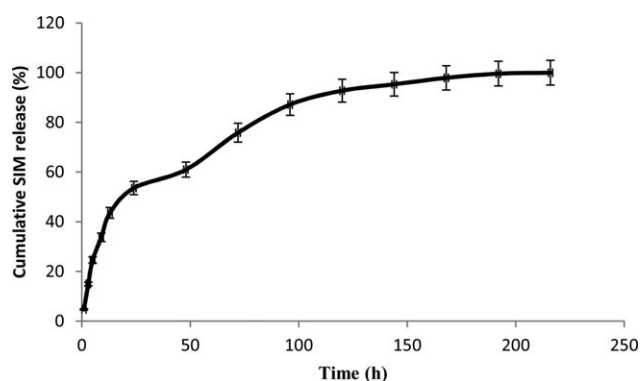


**Figure 7.** Drug release profile of SIM from PLGA NPs. Mean  $\pm$  standard deviation;  $n = 3$ .

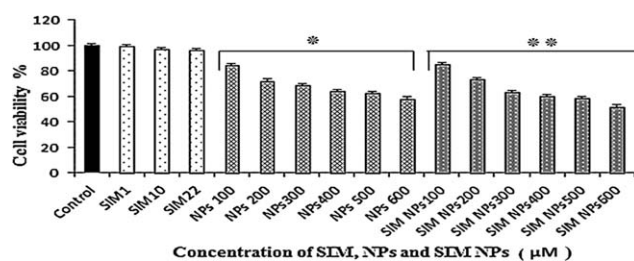


**Figure 8.** Cytotoxicity of simvastatin (SIM) (1, 10, 22  $\mu\text{M}$ ), poly(D, L-lactic-co-glycolide acid) (PLGA) nanoparticles (NPs) (100–600  $\mu\text{M}$ ) (\* $P < 0.001$ ), simvastatin-loaded poly(D, L-lactic-co-glycolide acid) nanoparticles (SIM-loaded PLGA NPs) (100–600  $\mu\text{M}$ ) (\*\* $P < 0.01$ ) assessed using the MTT assay ( $n = 3$ ).



preparation with minimum size showed appropriate encapsulation efficiency as well as release and cytotoxicity profiles.

#### ACKNOWLEDGMENTS

The authors thank Mehrdarou Pharmaceutical Company for providing Simvastatin as gift sample. This research has been supported by Tehran University of Medical Sciences and Health Services grant No 92-03-30-23890.

#### REFERENCES

1. Tiwari, G.; Tiwari, R.; Sriwastawa, B.; Bhati, L.; Pandey, S.; Pandey, P.; Bannerjee, S. K. *Int. J. Pharma. Investig.* **2012**, *2*, 2.
2. Kawashima, Y. *Adv. Drug Deliv. Rev.* **2001**, *47*, 1.
3. Shinde, A. J. M. H. *Der Pharma. Lett.* **2014**, *6*, 145.
4. Kumar, S.; Dilbaghi, N.; Saharan, R.; Bhanjana, G. *BioNano-Science* **2012**, *2*, 227.
5. Makadia, H. K.; Siegel, S. J. *Polymers* **2011**, *3*, 1377.
6. Reis, C. P.; Neufeld, R. J.; Ribeiro, A. J.; Veiga, F. *Nanomedicine* **2006**, *2*, 8.
7. Vauthier, C.; Bouchemal, K. *Pharm. Res.* **2009**, *26*, 1025.
8. Zarrabi, A.; Vossoughi, M. *Roznov Pod Radhostem Czech Republic EU* **2009**, *10*, 20.
9. Bock, N.; Woodruff, M. A.; Huttmacher, D. W.; Dargaville, T. R. *Polymers* **2011**, *3*, 131.
10. Lassalle, V.; Ferreira, M. L. *Macromol. Biosci.* **2007**, *7*, 767.
11. Sahoo, S.; Lee, W. C.; Goh, J. C. H.; Toh, S. L. *Biotechnol. Bioeng.* **2010**, *106*, 690.
12. Sridhar, R.; Ramakrishna, S. *Biomatter* **2013**, *3*, e24281.
13. Pastori, D.; Polimeni, L.; Baratta, F.; Pani, A.; Del Ben, M.; Angelico, F. *Dig. Liver Dis.* **2015**, *47*, 4.
14. Taylor, F.; Ward, K.; Moore, T. H.; Burke, M.; Davey, S. G.; Casas, J. P.; Ebrahim, S. *Cochrane Database Syst. Rev.* **2011**, CD004816.
15. Romana, B.; Batger, M.; Prestidge, A.; Colombo, C.; Sonvico, G. F. *Curr. Top. Med. Chem.* **2014**, *14*, 1182.
16. Soni, A.; Gadad, A.; Dandagi, P.; Mastiholmath, V.; Asian, J. *Pharmacology* **2011**, *5*, 57.
17. Patel, J. L.; Goyal, R. K. *Curr. Clin. Pharmacol.* **2007**, *2*, 217.
18. Amani, A.; York, P.; Chrystyn, H.; Clark, B. J. *Pharm. Res.* **2010**, *27*, 37.
19. Bourquin, J.; Schmidli, H.; van Hoogevest, P.; Leuenberger, H. *Eur. J. Pharm. Sci.* **1998**, *7*, 5.
20. Nasr, M. S.; Moustafa, M. A.; Seif, H. A.; El Kobrosy, G. *Alexandria Eng. J.* **2012**, *51*, 37.
21. Khan, I. Y.; Zope, P.; Suralkar, S. *Int. J. Eng. Sci. Innov. Technol.* **2013**, *2*, 210.
22. Zarchi, A. A. K.; Abbasi, S.; Faramarzi, M. A.; Gilani, K.; Ghazi-Khansari, M.; Amani, A. *Int. J. Biol. Macromol.* **2015**, *72*, 764.
23. Czitrom, V. *Am. Stat.* **1999**, *53*, 126.
24. Wang, B. B.; Wang, X. D.; Wang, T. H.; Lee, D. J. *Drying Technol.* **2015**, *33*, 406.
25. Xie, J.; Lim, L. K.; Phua, Y.; Hua, J.; Wang, C. H. *J. Colloid Interface Sci.* **2006**, *302*, 103.
26. Amsa, P.; Jagadeeswaran, T. S.; Sivakumar, M. T. *Int. J. Pharm. Pharm. Sci.* **2014**, *6*, 265.
27. Nath, S. D.; Son, S.; Sadiasa, A.; Min, Y. K.; Lee, B. T. *Int. J. Pharm.* **2013**, *443*, 87.
28. Jaworek, A. *Powder Technol.* **2007**, *176*, 18.
29. Aghajani, M.; Shahverdi, A. R.; Rezayat, S. M.; Amini, M. A.; Amani, A. *Pharm. Dev. Technol.* **2013**, *18*, 609.
30. Amini, M. A.; Faramarzi, M. A.; Mohammadyani, D.; Esmailzadeh-Gharehdaghi, E.; Amani, A. *J. Pharm. Innov.* **2013**, *8*, 111.
31. Hartman, R. P. A. B.; Camelot, D. J.; Marijnissen, D. M. A. J. C. M. *J. Aerosol. Sci.* **2000**, *31*, 65.
32. Ding, L.; Wang, L. T. C. *J. Control. Release* **2005**, *102*, 395.
33. Mura, S.; Hillaireau, H.; Nicolas, J.; Le Droumaguet, B.; Gueutin, C.; Zanna, S.; Tsapis, N.; Fattal, E. *Int. J. Nanomed.* **2011**, *6*, 2591.
34. Tandale, P.; Joshi, D.; Gaud, R. S. *Asian J. Biomed. Pharm. Sci.* **2011**, *1*, 13.
35. Wang, C. Z.; Fu, Y. C.; Jian, S. C.; Wang, Y. H.; Liu, P. L.; Ho, M. L.; Wang, C. K. *J. Colloid Interface Sci.* **2014**, *432*, 190.
36. Mahapatro, A. S. D. *J. Nanobiotechnol.* **2011**, *9*, 55.
37. Wiesbauer, F.; Kaun, C.; Zorn, G.; Maurer, G.; Huber, K.; Wojta, J. *Br. J. Pharmacol.* **2002**, *135*, 284.
38. Medina, R. J.; O'Neill, C. L.; Devine, A. B.; Gardiner, T. A.; Stitt, A. W. *PloS One* **2008**, *3*, e2584.
39. Gauthaman, K.; Manasi, N.; Bongso, A. *Br. J. Pharmacol.* **2009**, *157*, 962.